CHAPTER FIVE:
THE RESPONSE OF *gol/gol* CELLS TO DNA DAMAGE

5.1 INTRODUCTION

Numerous studies have demonstrated that *BRCA1* mutations in both mouse and human cells confer hypersensitivity to DNA damage (reviewed in Kerr and Ashworth, 2001; Deng and Wang, 2003). Previous studies of the role of BRCA1 in DNA damage have not generally attempted to designate the specific domains required for resistance to a damaging agent, and in many cases, cell lines with known secondary mutations (*e.g.* tumour-derived cell lines) have been used to demonstrate sensitivity. Various damaging agents have been used in such assays; one common one is γ-irradiation. Most reports agree that the entire BRCA1 protein appears to be necessary for a normal response to this mutagen; cells homozygous for deletions of exon 11, or for deletions of the N- or C-termini are all hypersensitive to γ-irradiation (Shen, 1998; Abbott, 1999; Ruffner, 2001; Zhou, 2003). The second main goal of this project was to determine the sensitivity of *gol/gol* ES cells to various DNA damaging agents. As the *gol* allele is predicted to give rise to a protein lacking the N-terminal RING domain (referred to here as $Brca1^{gol}$), these experiments may help uncover the importance of the N-terminus in the response of Brca1 to DNA damage.

5.1.1 Mutagenic agents used in these experiments

gol/gol ES cells were exposed to four mutagenic agents: γ-irradiation (primary lesion: double-strand breaks), mitomycin C (MMC; primary lesion: interstrand cross-links), UV irradiation (primary lesion: mutated bases), and H_2O_2 (oxidative damage resulting in mutated bases). The methods used to repair such lesions were discussed in sections 1.11.3 and 1.11.4. The experiments described in this chapter indicate that *gol/gol* ES cells are not hypersensitive to mutagens which cause base damage, but do have a defect in double-strand break repair (DSBR). Once this result was obtained, the efficiencies of both homologous recombinational repair (HRR) and non-homologous end joining (NHEJ), the two major forms of DSBR, were additionally tested in *gol/gol* cells.

5.1.2 Immunolocalization of Brca1^{gol}

BRCA1 is a nuclear protein which is hyperphosphorylated and forms nuclear foci following DNA damage (Scully, 1996). Although the precise function of these foci is unknown, they contain several other proteins known to be involved in DNA repair, such as RAD51, BRCA2, BLM, and RAD50, and are likely to be involved in the sensing and/or repair of DNA damage (see section 1.11.3 for a summary) (Scully, 1997c; Chen, 1998; Wang, 2000b). It is currently unknown which domains of BRCA1 are required for damage-induced focus formation, although human HCC1937 cells, which carry a C-terminal truncated version of BRCA1, do not exhibit nuclear foci after DNA damage, while MEFs carrying only the ΔX.11 isoform of Brca1 do form damage-induced foci (Zhong, 1999; Wu, 2000; Huber, 2001).

In this study, the cellular localization of the Brca1^{gol} protein, which is thought to lack all or most of the N-terminal RING domain, was determined by immunolocalization using an antibody raised against an epitope from the C-terminus of the mouse protein. The immunolocalization patterns of Brca1^{gol} and wildtype Brca1 are very similar; both are observed in the nucleus and cytoplasm, and nuclear foci are seen in undamaged cells of both genotypes. However, the amount of cytoplasmic localization is higher than has generally been observed, and the overall localization pattern is fairly punctate. Following UV exposure, to which the *gol/gol* cells are not hypersensitive, damage-induced nuclear foci are observed in wildtype and *gol/gol* cells. Damage-induced nuclear foci are also observed following treatment with γ-irradiation, to which *gol/gol* cells are hypersensitive, but a proportion of γ-irradiated *gol/gol* cells also appear to have large aggregates of Brca1^{gol} protein.

5.2 RESULTS

5.2.1 *gol/gol* ES cells grow normally compared to wildtype ES cells

To ascertain if *gol/gol* ES cells have a growth defect, the doubling times of *gol/gol* and wildtype ES cells in culture were established. Duplicate samples

of each cell line were counted every twelve hours for seven days. Figure 5.1 shows the resulting growth curves. Doubling times were calculated using the formula $DT=(t_1-t_0)/3.3 \log_{10}(N_1/N_0)$, where t_0 and N_0 represent the first time point and the number of cells at the first time point, respectively, and t_1 and N_1 represent a second time point and the number of cells at that time, respectively. Doubling times calculated for the period of log-phase growth (a straight line on a semi-log plot) were: 25 hours (wildtype), 24 hours (*gol/gol*) and 25 hours (*gol/gol 2*). Doubling times calculated over the entire seven days were: 26 hours (wildtype), 28 hours (*gol/gol*), and 30 hours (*gol/gol 2*). In either case, these are not appreciably different. This assay was only performed once. The same two *gol/gol* ES cell lines were used in the rest of the experiments described in this chapter.

A growth curve alone does not address potential changes in cell-cycle timing or the possibility of a block or delay in one part of the cell cycle. This has a bearing on the DNA damage assays described in this chapter, as the repair mechanism of DSBs depends in part on the phase of the cell cycle (see section 1.11.3.1.1). If *gol/gol* cells have a delay in going into S phase, DSBs may be more likely to be repaired by NHEJ, meaning that repair overall may be more error prone (and more detrimental), or that later assays used to determine the efficiency of HR and NHEJ in mutant cells would need to be interpreted with this bias in mind. Alternatively, if mutant cells have a shorter doubling time coupled with an increased amount of cell death, their growth curve might resemble that of wildtype cells. To partially allay these concerns, the cell-cycle profile of wildtype and *gol/gol* ES cells was determined by harvesting cells while in log-phase growth, labeling them with propidium iodide to measure DNA content, and performing flow cytometric analysis (see section 2.2.5.1 for details; flow sorting was performed by Bee Ling Ng of the Sanger Institute). Figure 5.1b shows overlapped cell-cycle profiles from wildtype and the two *gol/gol* ES cell lines. Markers show the regions used to calculate the percentage of cells in each phase; in all cases, the proportions were not different (values shown are an average of three experiments).

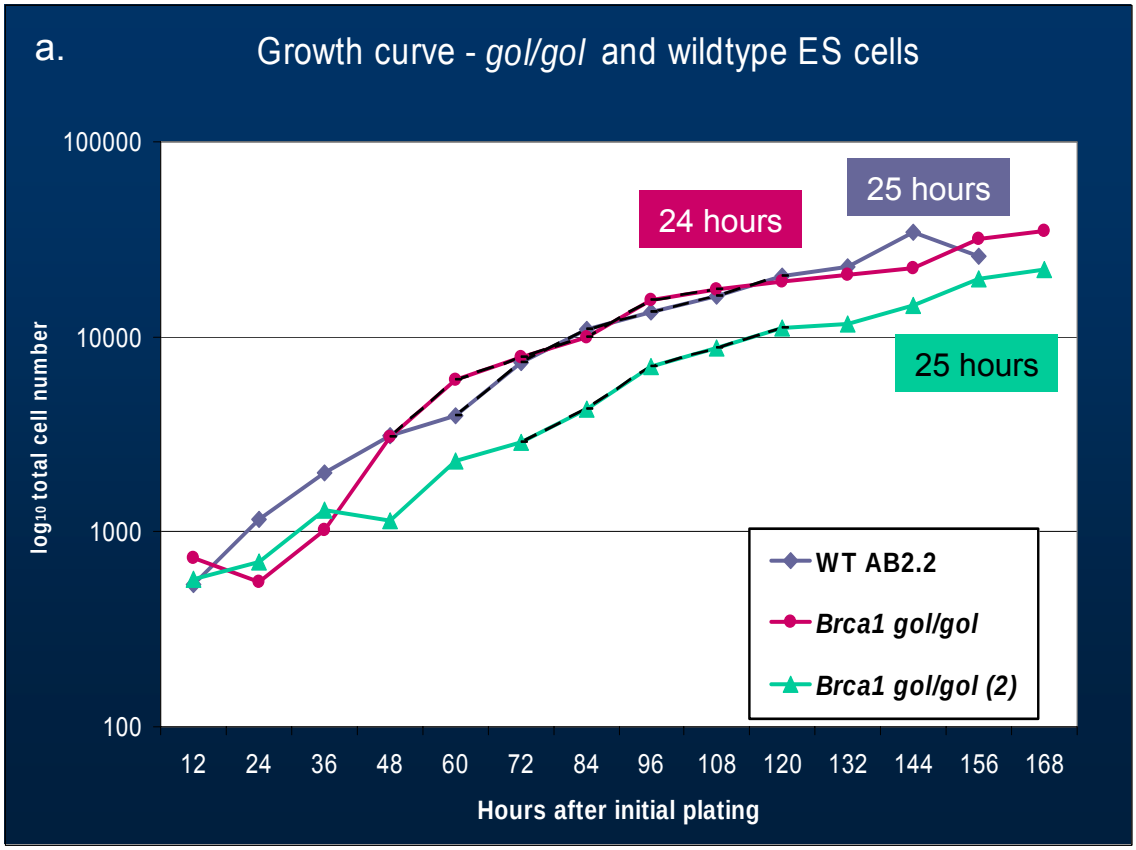

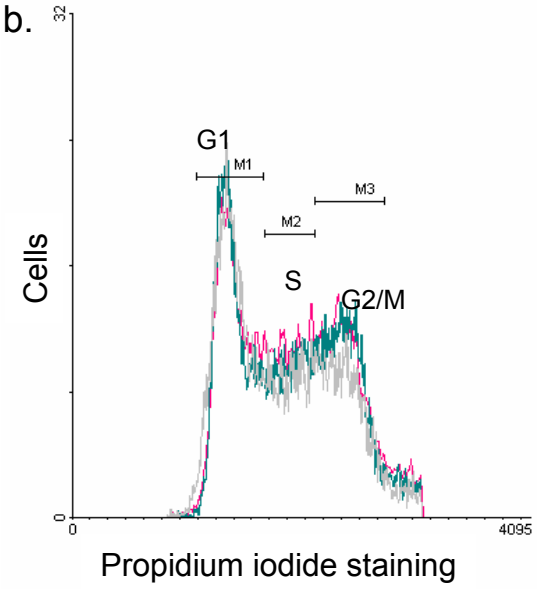

c.

Percentage of cells in each phase

	G1	S	G2/M
Wildtype (pink)	38 (1.25)	25 (0.94)	34 (1.63)
gol/gol (green)	42 (2.45)	25 (0.82)	31 (2.05)
gol/gol (2) (grey)	44 (2.08)	25 (1.00)	29 (2.08)

Figure 5.1: Growth curves and cell sorting of *gol/gol* and wildtype ES cells. **a.** Doubling times, as calculated from the log-phase period of growth (marked by dashed black lines on the curves), are indicated on the graph (see text for doubling time formula). Overall doubling times, calculated over the entire seven days were: 26 hours (wildtype), 28 hours (*gol/gol*), and 30 hours (*gol/gol(2)*). This assay was only performed once. **b.** Overlain cell-cycle profiles of wildtype (pink), *gol/gol* (green), and *gol/gol(2)* (grey) cells harvested in log-phase growth and stained with propidium iodide for DNA content. 20,000 cells were counted per cell line. A representative overlay is shown. **c.** Sorting experiments were done in triplicate and the averaged percentage of cells in various phases is shown (standard deviation in parentheses).

This experiment indicates that *gol/gol* ES cells do not appear to accumulate in one phase of the cell cycle, but it does not show whether cells with a S phase amount of DNA are actively synthesizing DNA. This was not determined, but could be done by pulse-labeling the cells with the thymidine analogue BrdU prior to harvest. As BRCA1 is known to have roles in checkpoint control, determination of the cell-cycle kinetics of the *gol/gol* cell lines may provide useful data about the mechanism of the defect in these cells.

5.2.2 *gol/gol* ES cells are not hypersensitive to UV treatment or H_2O_2-induced oxidative stress

Treatment of *gol/gol* ES cells with UV irradiation or H_2O_2 at a range of doses indicated that their colony-forming efficiency following treatment with these mutagens does not differ from that of wildtype cells. Figures 5.2 (UV) and 5.3 (H_2O_2) show the effect of these mutagens on the colony-forming ability of wildtype or *gol/gol* ES cell lines, normalized against the colony-forming ability of non-treated controls (plating efficiency at the “0” dose was thus set at “1”). All assays were performed at least in triplicate, with the error bars representing one standard deviation of the mean.

5.2.3 *gol/gol* ES cells are hypersensitive to γ-irradiation and mitomycin C (MMC) treatment

Exposure of *gol/gol* ES cells to γ-irradiation or the cross-linking agent MMC revealed that *gol/gol* ES cells are hypersensitive to both of these mutagens when compared to either wildtype or heterozygous ES cells. Figures 5.4 (γ-irradiation) and 5.5 (MMC) show the effects of these mutagens on the colony-forming ability of ES cells, normalized against that of non-treated controls. All assays were performed at least in triplicate, with the error bars representing one standard deviation of the mean.

At lower doses of γ-irradiation or MMC (100 or 250 rads or up to 1 μM MMC), *gol/gol* and wildtype ES cells have similar colony-forming abilities. For both mutagens, this similarity ends around the doses which kill ~50% of the

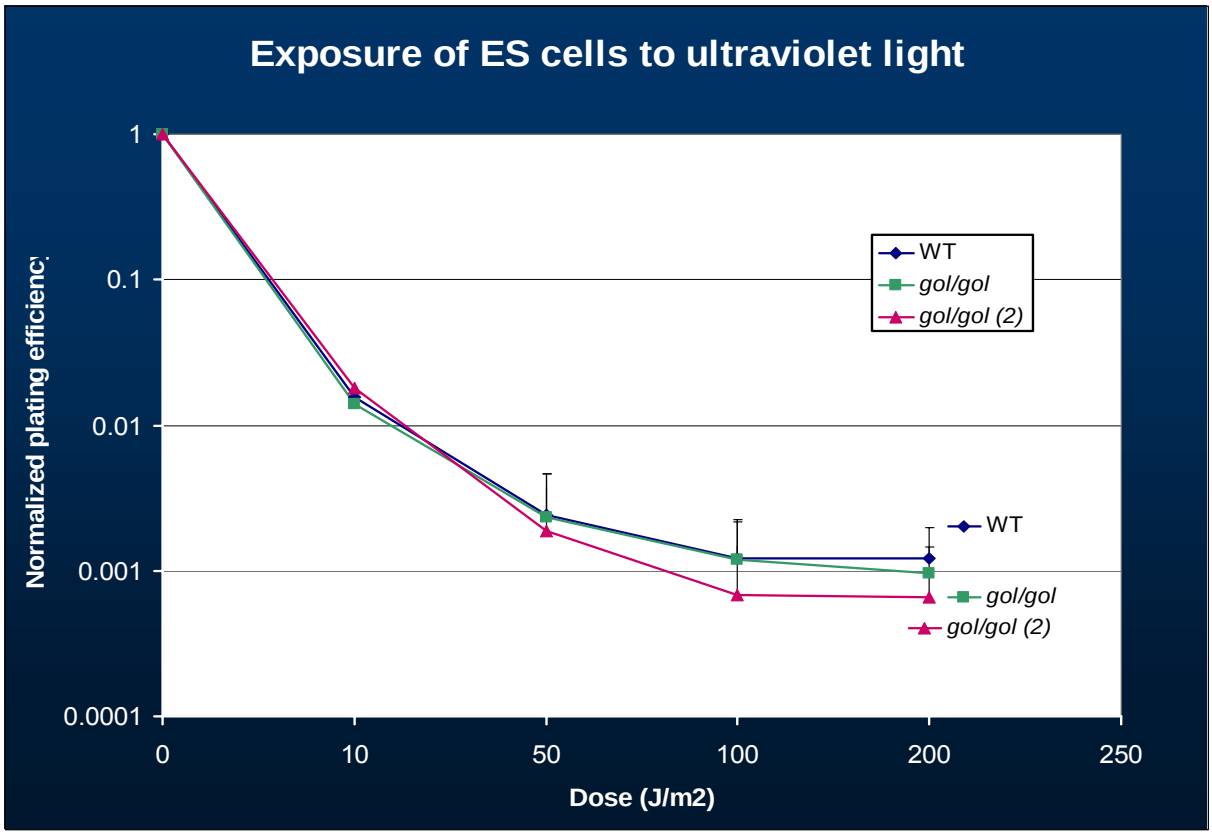

Figure 5.2: Plating efficiency of ES cells following UV exposure. *gol/gol*, *+/gol*, or wildtype ES cells were exposed to 0, 10, 50, 100, or 200 J/m^2 UVC. (254 nm at a power level of 40 watts/m^2). Plating efficiencies were normalized against the plating efficiency of non-treated controls. All assays were performed at least in triplicate. Error bars represent one standard deviation of the mean, but are only shown in the upward direction to simplify the graph.

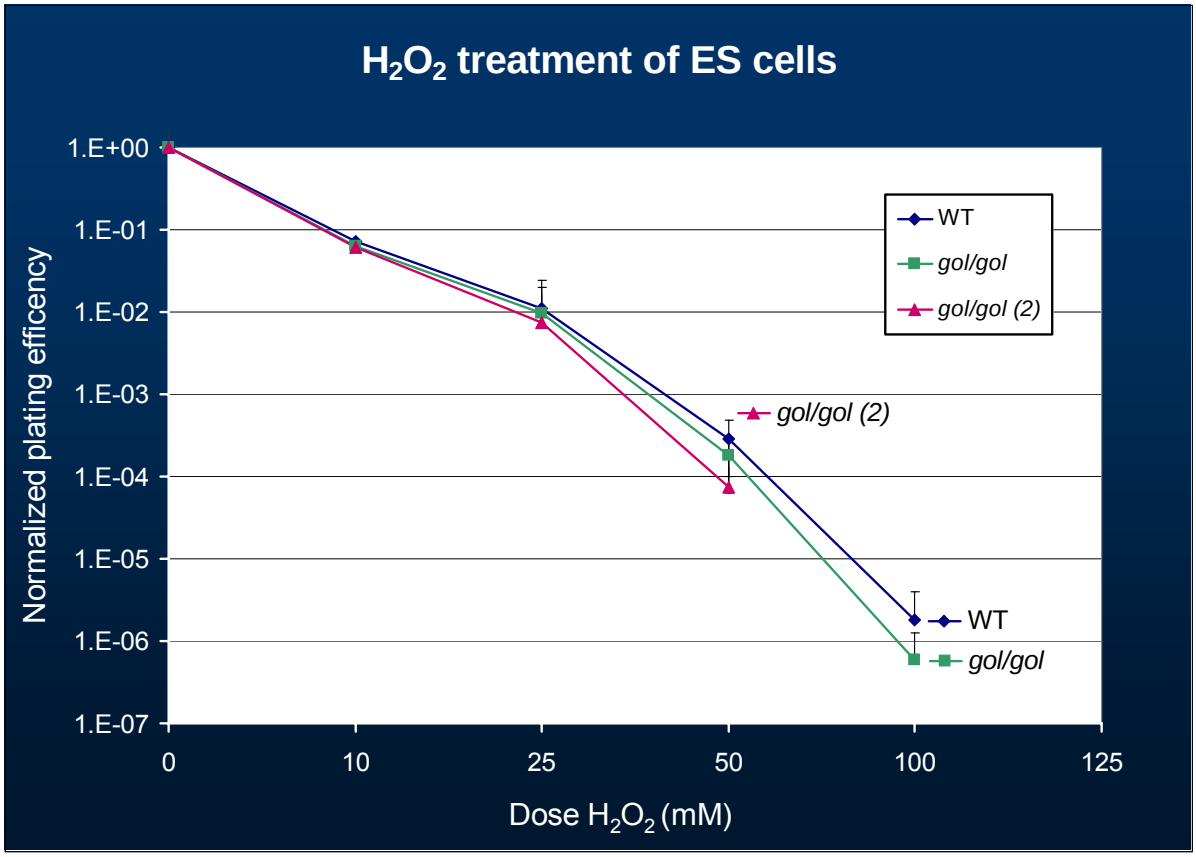

Figure 5.3: Plating efficiency of ES cells following H_2O_2 exposure. *gol/gol*, *+/gol*, or wildtype ES cells were exposed to 0, 10, 25, 50, or 100 mM H_2O_2 for 15 minutes. Plating efficiencies were normalized against the plating efficiency of non-treated controls. All assays were performed at least in triplicate. Error bars represent one standard deviation of the mean, but are only shown in the upward direction to simplify the graph.

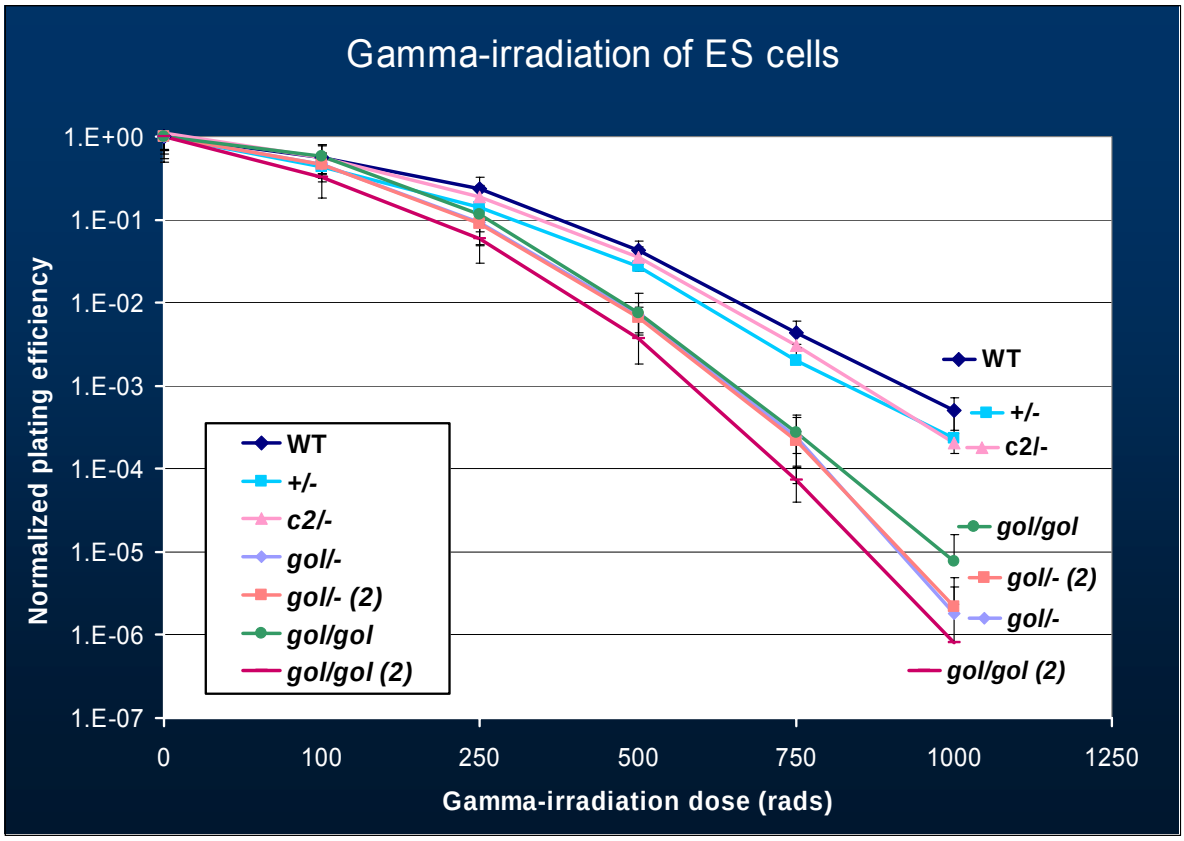

Figure 5.4: Plating efficiency of ES cells following γ-irradiation.
ES cells of the indicated genotypes were exposed to 0,100, 250, 500, 750, or 1000 rads of γ-irradiation (dose rate: 789 rads/minute). Plating efficiencies were normalized against the plating efficiency of non-treated controls. All assays were performed at least in triplicate. Error bars represent one standard deviation of the mean.

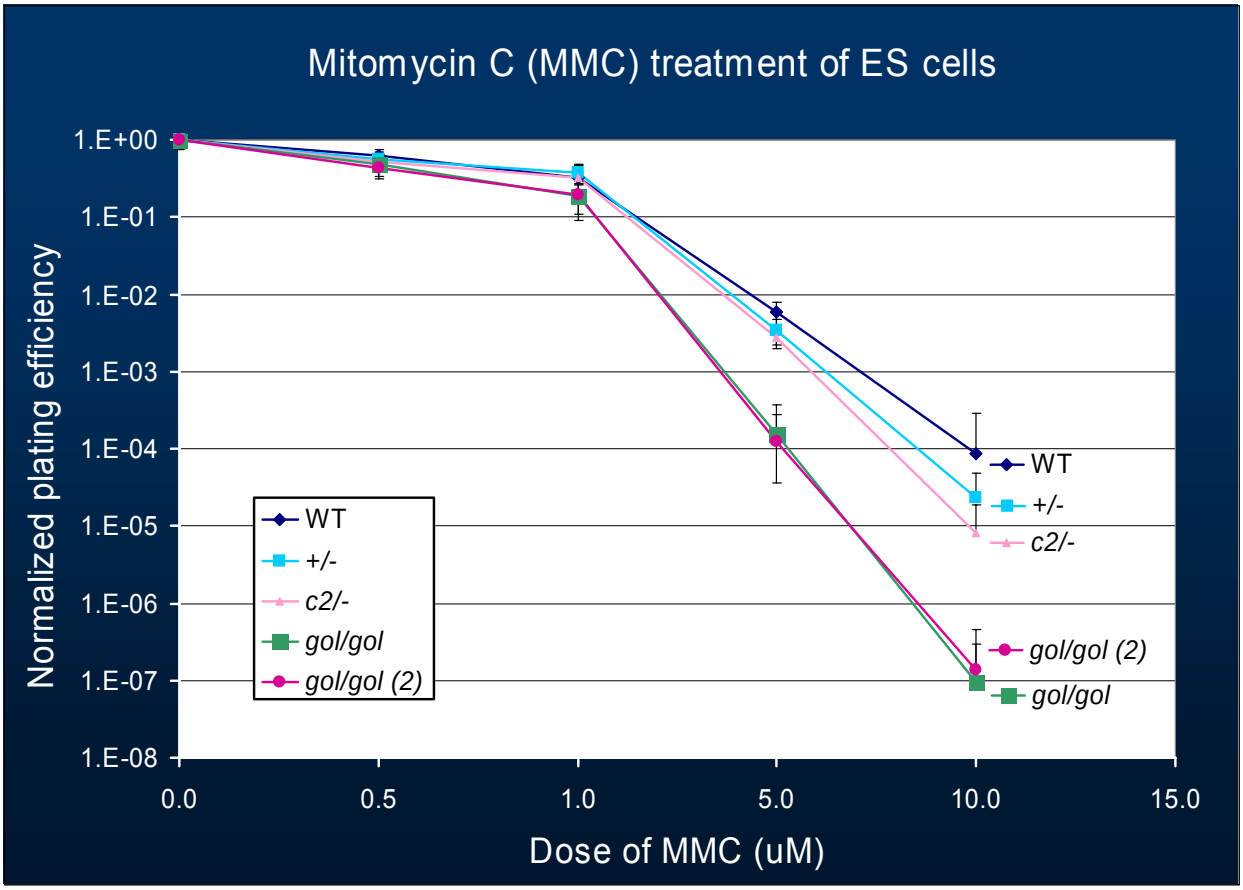

Figure 5.5: Plating efficiency of ES cells following MMC treatment. ES cells of the indicated genotype were exposed to 0, 0.5, 1, 5, or 10 μM MMC for four hours. Plating efficiencies were normalized against the plating efficiency of non-treated controls. All assays were performed at least in triplicate. Error bars represent one standard deviation of the mean.

wildtype cells (100-250 rads, or 0.5–1 μM MMC). At higher doses, there is an increasingly large difference between the survival of *gol/gol* or *–/gol* and control cell lines. Colonies formed from *gol/gol* or *–/gol* cells given higher doses of MMC or γ-irradiation were consistently smaller than those formed by similarly-treated wildtype cells, and were routinely cultured for two extra days to allow the colonies to be scored more easily.

As discussed in section 1.11.3, the characteristic lesions formed after γ-irradiation or MMC treatment are repaired by DSBR mechanisms. The two major forms of DSBR are HRR and NHEJ (see Figure 1.13). The DSBR defect observed in *gol/gol* ES cells prompted further experiments to assess the efficiency of homologous recombination and NHEJ in these cells.

5.2.4 *gol/gol* ES cells have a small deficiency in gene-targeting efficiency

Homologous recombination repair is commonly tested one of several methods, including by I-SceI assay (I-SceI assays add a recognition site for the rare-cutting I-SceI endonuclease to the cell, either by direct integration into the genome or on a plasmid; transfection of the nuclease into cells generates the break. Generally, accurate repair of the break is measured by reconstitution of a selection cassette), pulsed-field gel electrophoresis, or by measuring the efficiency of gene targeting. A number of groups within the BRCA field have used gene targeting to look at HRR (Essers, 1997; Rijkers, 1998; Jasin, 2002). In studies using this and other assays, the results of the two, while differing in fold-induction, generally show the same trend.

The efficiency of homologous recombination in *gol/gol* and wildtype ES cells was tested by gene targeting using both a replacement vector (for *Gdf-9*, a gift from Marty Matzuk of Baylor College of Medicine, Houston, TX (Dong, 1996)), and an insertion vector (for *Melk*, isolated from the 5' *Hprt* targeting vector library (Zheng, 1999a) by a colleague, Jyh-Yih Chen). Screening for correctly-targeted colonies was done by mini-Southern (Figure 5.6). Figure

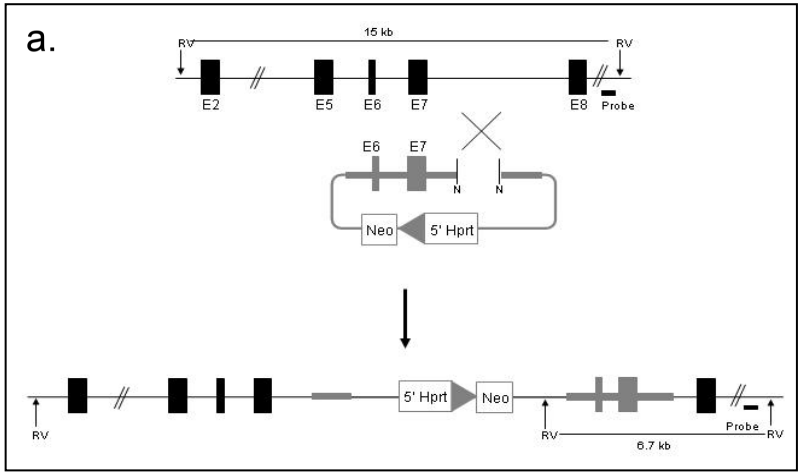

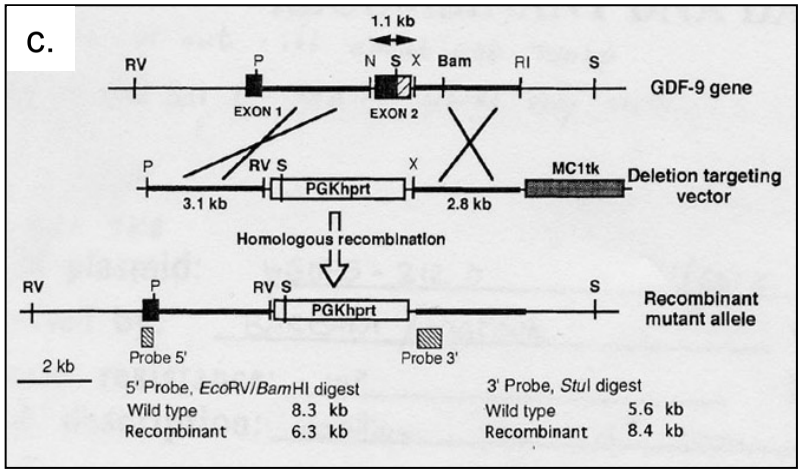

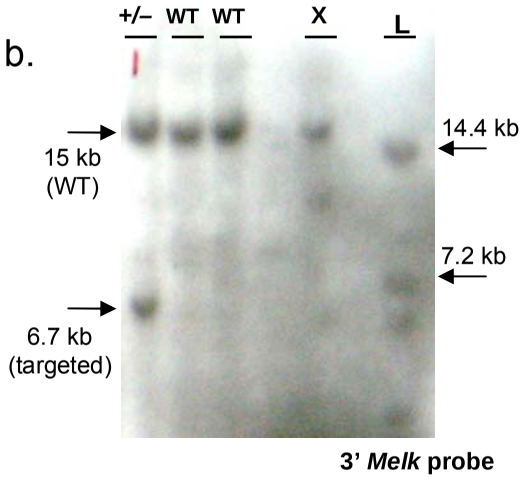

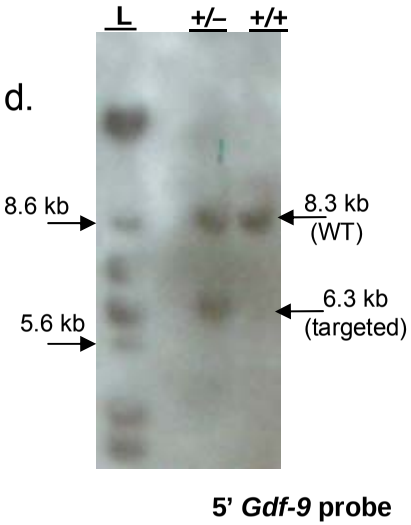

Figure 5.6: Targeting *Gdf-9* and *Melk*. **a.** The *Melk* targeting vector and probe schematic, modified from a diagram provided by Dr. Louse van der Weyden. **b.** Representative mini-Southern blot showing targeted and non-targeted *Melk* clones. **c.** The *Gdf-9* targeting vector and probe schematic, taken from (Dong, 1996). **d.** Representative mini-Southern blot showing targeting and non-targeted *Melk* clones. L=ladder, WT=wildtype, RV=*Eco*RV, N=*Nde*I, X=incorrect targeting.

5.7a shows that the targeting frequency of *gol/gol* ES cells is lower than that of wildtype cells for both genes. The average of three experiments is plotted; error bars represent one standard deviation from the mean. A two-tailed t-test indicates that the difference between the targeting efficiency of either *gol/gol* ES cell line and the wildtype control is statistically significant (a *p*-value of less than 0.05 is considered significant). However, once these values are corrected for random integration (as measured by the total number of drug-resistant colonies resulting from an entire *Melk* electroporation, Figure 5.7b), the absolute targeting frequencies of *gol/gol* and wildtype cells are more similar (Figure 5.7c), and although they are still lower than that of wildtype cells, the difference is smaller, ranging from 1.2-fold to 5.6-fold lower.

5.2.5 *gol/gol* ES cells have an increase in NHEJ efficiency

Assaying NHEJ is commonly done by one of several methods – I-SceI rejoining, direct integration of plasmids, plasmid-based transfection assays (in cells or using cell-free extracts), pulsed-field gel electrophoresis-based measurement of repair kinetics, or by measuring the response to retroviral insertion (Daniel, 1999; Moynahan, 1999; Li, 2001; Willers, 2002; Zhong, 2002a; Zhong, 2002b).

The NHEJ efficiency of *gol/gol* ES cells was tested using the gene trap vector pGT designed by Dr. William Skarnes (Wellcome Trust Sanger Institute, Hinxton, UK). The trap cassette consists of a promoterless *β-geo* gene (a fusion of *Neo* and *β-gal*) proceeded by a splice acceptor from the mouse *engrailed-2* gene (Figure 1.17). *β-geo* lacks an ATG start site, and must be successfully spliced into a transcript before it can be expressed. pGT is randomly integrated into the genome by direct electroporation into ES cells, meaning that this assay for random integration does not depend on any intermediate steps, as would be the case in retroviral-mediated delivery of a gene trap cassette (Skarnes, 2000).

Both of the *gol/gol* ES cell lines have an increased efficiency of NHEJ as measured by gene trapping (Figure 5.8). A two-tailed t-test indicates that this

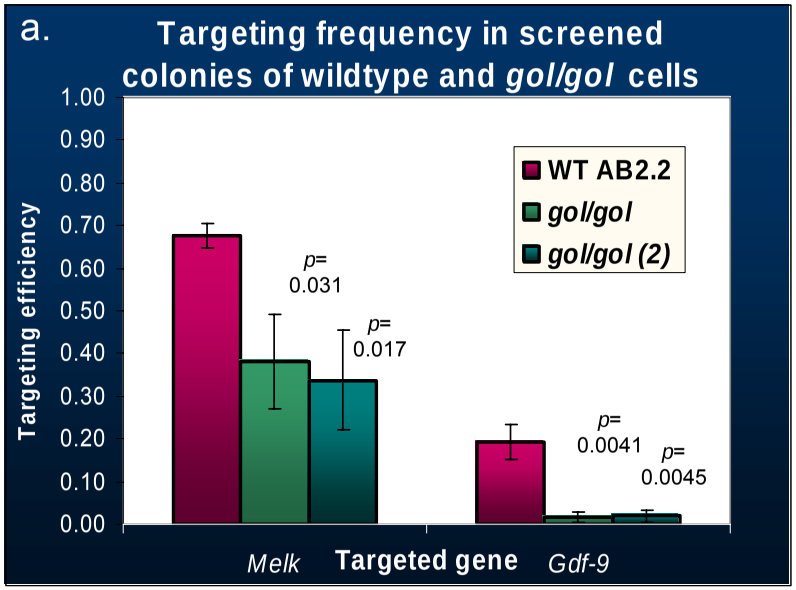

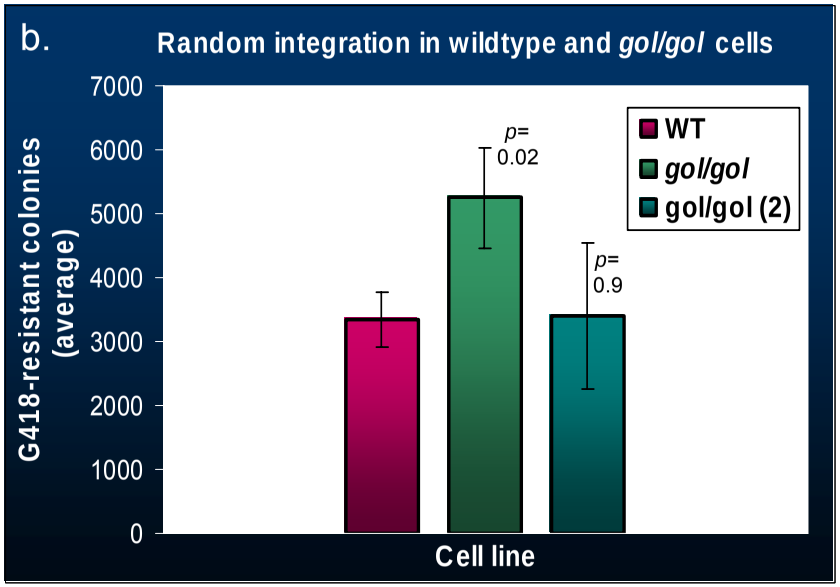

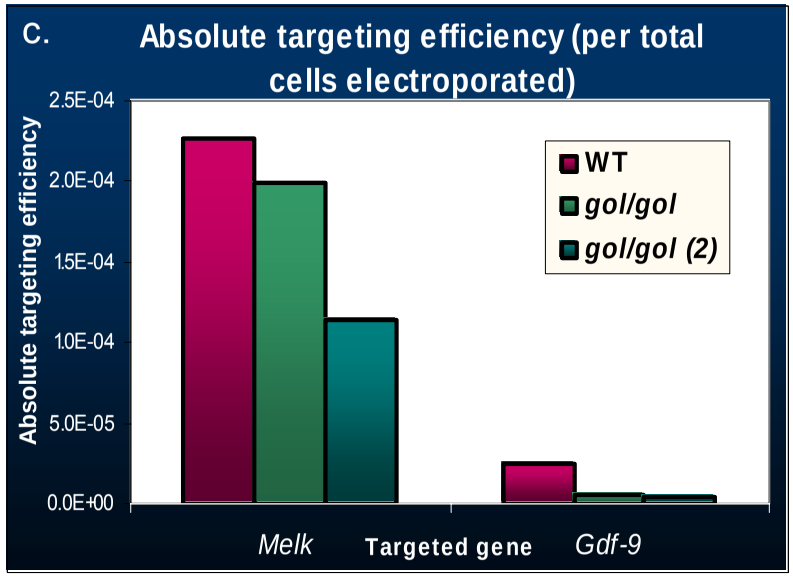

Figure 5.7: Targeting efficiencies of wildtype and *gol/gol* ES cells. **a.** The average targeting efficiency of three targeting experiments per gene per cell line is graphed. **b.** Random integration of the *Melk* targeting vector in WT and *gol/gol* ES cells. The average number of drug-resistant colonies from three experiments is graphed. **c.** The absolute targeting efficiency of each cell line (per 10^7 cells electroporated), taking both the targeting frequency and the amount of random integration into account.
Error bars represent one standard deviation of the mean.
p-values were calculated using a two-tailed t-test and compare the indicated *gol/gol* sample to the wildtype control.
WT= wildtype.

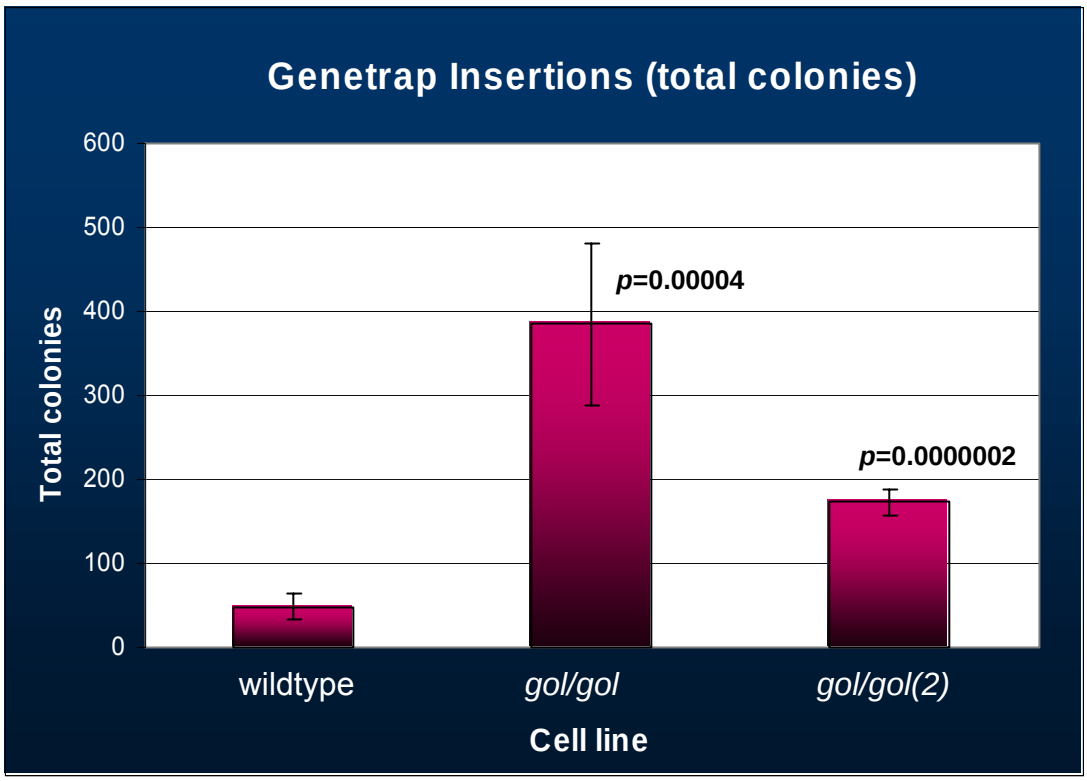

Figure 5.8: NHEJ efficiencies of wildtype and *gol/gol* ES cells.
The average total colony number from three experiments per cell line is graphed. Error bars indicate the standard deviation. Statistical significance of the result from each *gol/gol* cell line compared to the wildtype control was measured by a two-tailed t-test. *p*-values are shown (a *p*-value less than 0.05 is considered significant).

increase is statistically significant. The average of three experiments is plotted; error bars represent one standard deviation from the mean.

5.2.6 Brca1^{gol} cellular localization

In order to determine if Brca1^{gol} is found in the nucleus, immunolocalization studies were performed using *gol/gol* and wildtype cells (immunolocalization and confocal microscopy were performed by Michal Goldberg of the Wellcome Trust/Cancer Research UK, Cambridge). As ES cells are very small and a *gol/gol* mouse model did not yet exist from which MEFs could be generated, *gol/gol* and wildtype ES cells were differentiated in culture as described previously (Robertson, 1987) to provide larger cells. The antibody used in these studies was obtained from a commercial vendor (M-20, from Santa Cruz Biotechnology), raised to a peptide from the C-terminus of murine Brca1. Previous immunolocalization studies using this antibody have demonstrated a nuclear and cytoplasmic localization profile of Brca1, similar to results obtained with other antibodies (Bachelier, 2000). The specificity of this antibody has been at least partially demonstrated in a study designed to test the specificity of a new BRCA1 antibody: the new antibody was used in an immunoprecipitation experiment, then the immunoprecipitates were subjected to Western blotting and probed with a panel of commercially available BRCA1 antibodies. M-20 performed identically to the other BRCA1 antibodies, including the widely-used Ab-1 antibody, but Western blot evidence shows that all the antibodies recognize not only the wildtype and ΔX.11 forms of Brca1 but at least two other bands which may be non-specific or may arise from alternative splicing of the *Brca1* gene (Zhang, 1997).

As indicated in Figure 5.9, Brca1 is located in both the nucleus and the cytoplasm in both wildtype (5.9a) and *gol/gol* (5.9b) cells. In addition, Brca1 nuclear foci are observed in undamaged cells of both genotypes (Figure 5.10), in accordance with what has been observed in numerous other BRCA1 immunolocalization studies (*e.g.* (Scully, 1997c; Wang, 2000b; Huber, 2001)). The amount of focus formation may be lower than it appears, as the overall punctate appearance of the immunolocalization pattern may lead to an

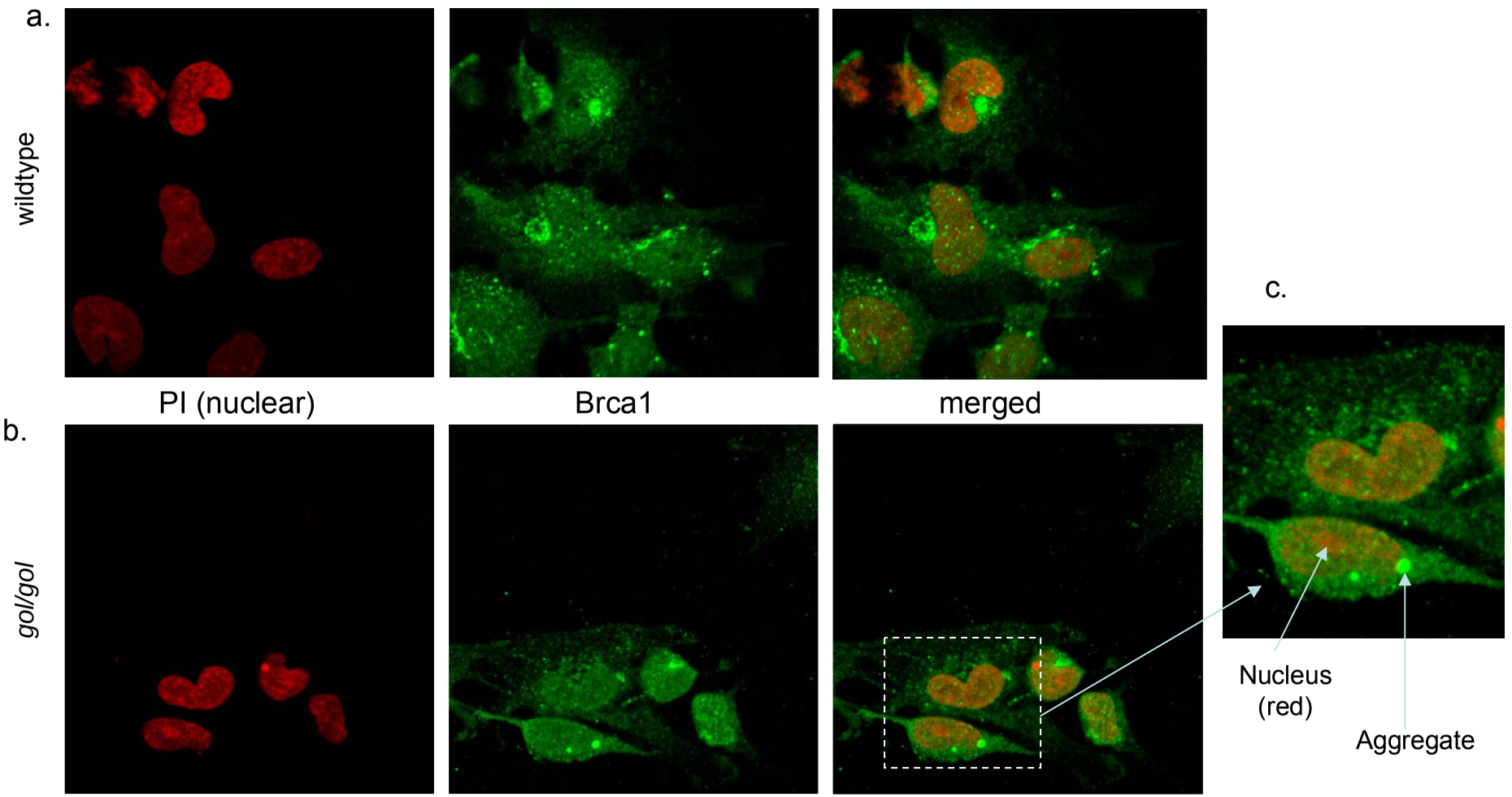

Figure 5.9: Nuclear localization of Brca1 in *gol/gol* and wildtype cells.
a. Wildtype cells. **b.** *gol/gol* cells. **c.** Zoom-in on one *gol/gol* cell to show an aggregate in an untreated cell. Brca1 staining is shown in green, nuclear staining with propidium iodide (PI) in red. Immunlocalization and confocal microscopy were performed by Michal Goldberg (see Methods). The Brca1 antibody M-20 (Santa Cruz) was used.

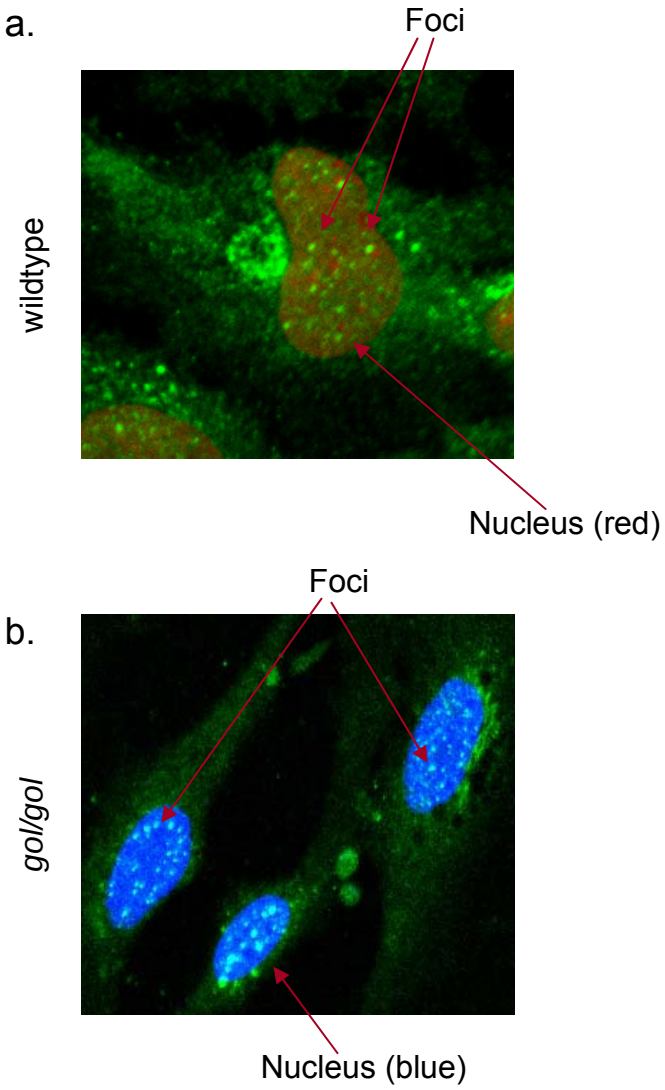

Figure 5.10: Nuclear foci in undamaged cells.
a. Wildtype cells. Brca1 staining is shown in green, nuclear staining with propidium iodide (PI) in red.
b. *gol/gol* cells. Brca1 staining is shown in green, nuclear staining with TOTO-3 iodide in blue. Both nuclear and cytoplasmic localization of Brca1 is observed, and nuclear foci are observed in cells of both genotypes. Immunlocalization and confocal microscopy were performed by Michal Goldberg (see Methods). The Brca1 antibody M-20 (Santa Cruz) was used.

overestimation of focus formation. Some *gol/gol* cells additionally have larger aggregates of protein near the nucleus or in the cytoplasm, but such aggregates were also seen in wildtype cells (inset Figure 5.9 and Table 5.1). Oddly-shaped nuclei are a normal characteristic of differentiated cells and are seen in both the *gol/gol* and wildtype cell lines. It is possible that levels of Brca1 protein may be higher in *gol/gol* cells, although no attempt at formal quantification was made. The level of cytoplasmic Brca1 localization, although consistent between wildtype and *gol/gol* cell lines, is higher than has been observed in other studies, and overall localization is fairly punctate. These observations are not constant with previous immunolocalization studies, and the presence of aggregates has not been reported previously. These discrepancies may result from the use of differentiated cells, which have not been used in previous studies, or from the antibody used. As discussed above, the antibody may recognize non-specific polypeptides, and before this experiment can be interpreted further, either use of another antibody, or a repeat of the experiment but using competitor Brca1 peptide to assess the specificity of the antibody should be done.

5.2.7 Localization patterns of Brca1^{gol} and wildtype Brca1 differ after γ-irradiation but are similar following UV treatment

The localization of Brca1 in nuclear foci following various forms of DNA damage is well-documented (Scully, 1996; Scully, 1997b). In this study both normal and damage-induced Brca1 nuclear foci were observed. Following exposure to UV irradiation, such foci were seen in a similar percentage of *gol/gol* and wildtype cells (Figure 5.11/Table 5.1). As mentioned previously, though the overall punctate appearance of the immunolocalization pattern may lead to an overestimation of the number of foci formed.

Following γ-irradiation, both *gol/gol* and wildtype cells also exhibit nuclear foci (Figure 5.12). However, ~25% of *gol/gol* cells have large, generally perinuclear, aggregates of protein (inset, Figure 5.12 and Table 5.1). These aggregates are rarely observed in UV-treated cells of either genotype, or in γ-irradiated wildtype cells. About 10% of untreated wildtype and 16% of

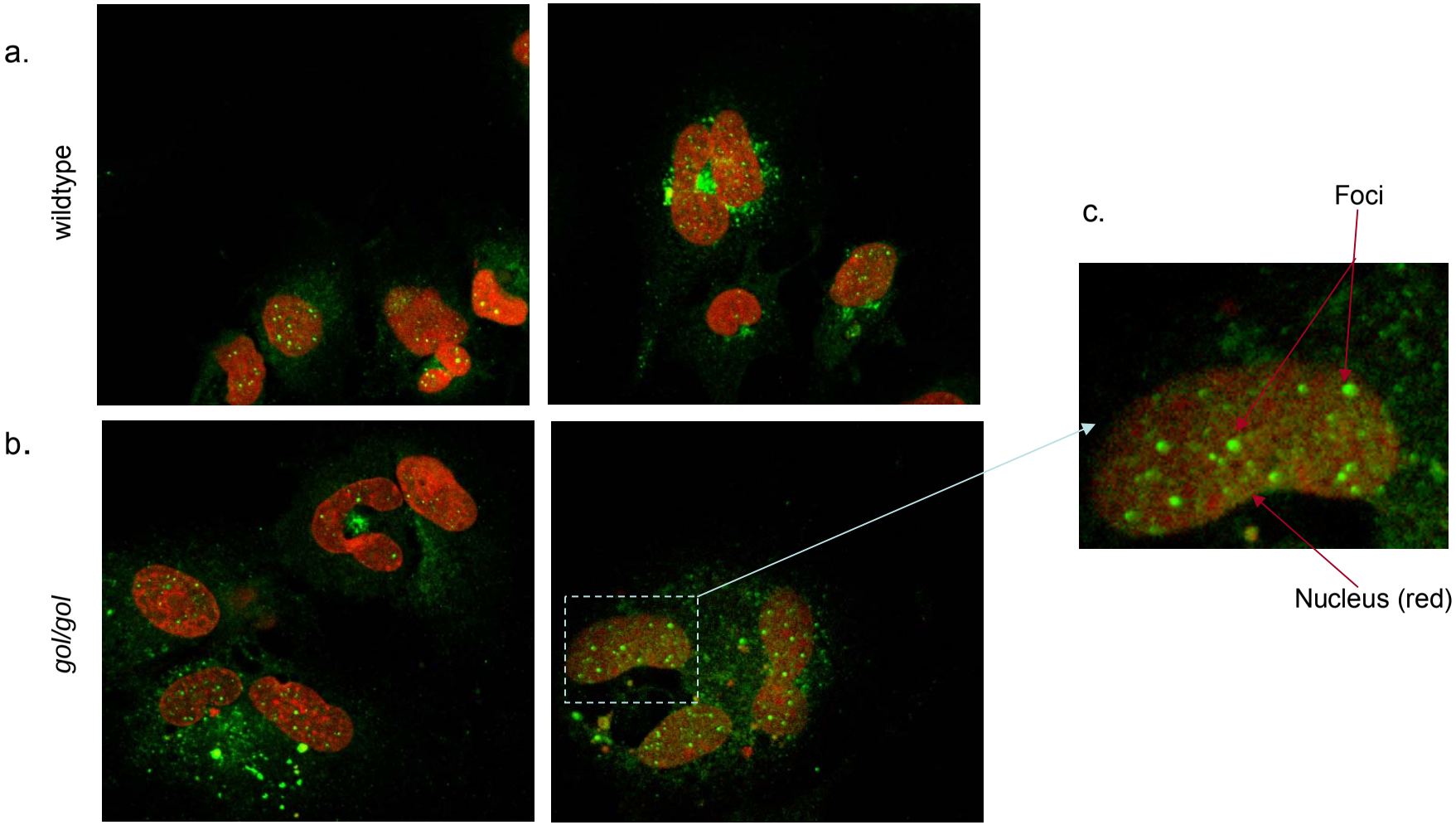

Figure 5.11: Nuclear localization of Brca1 in *gol/gol* and wildtype cells following UV exposure.
a. Wildtype cells. **b.** *gol/gol* cells**. c.** Zoom-in on a single *gol/gol* cell to show nuclear foci. Brca1 staining is shown in green, nuclear staining with propidium iodide (PI) in red; all images are shown as merges of both stains. Immunlocalization and confocal microscopy were performed by Michal Goldberg (see Methods). The Brca1 antibody M-20 (Santa Cruz) was used.

Table 5.1: Foci and aggregate formation in *gol/gol* or wildtype cells.
Foci and aggregates in *gol/gol* or wildtype cells, both untreated or following exposure to ultraviolet (UV)- or γ-irradiation. Nuclei were scored positive for foci if six or more foci were observed, and positive for aggregates if one large or several smaller aggregates were present.

Cell line	Treatment	Nuclei	Foci	Percentage of cells with foci	Aggregates	Percentage of cells with aggregates
Wildtype	none	117	46	39	12	10
gol/gol	none	89	18	20	14	16
Wildtype	γ-irradiation	102	48	47	2	2
gol/gol	γ-irradiation	51	31	61	13	25
Wildtype	UV	37	29	78	1	3
gol/gol	UV	35	24	69	1	3

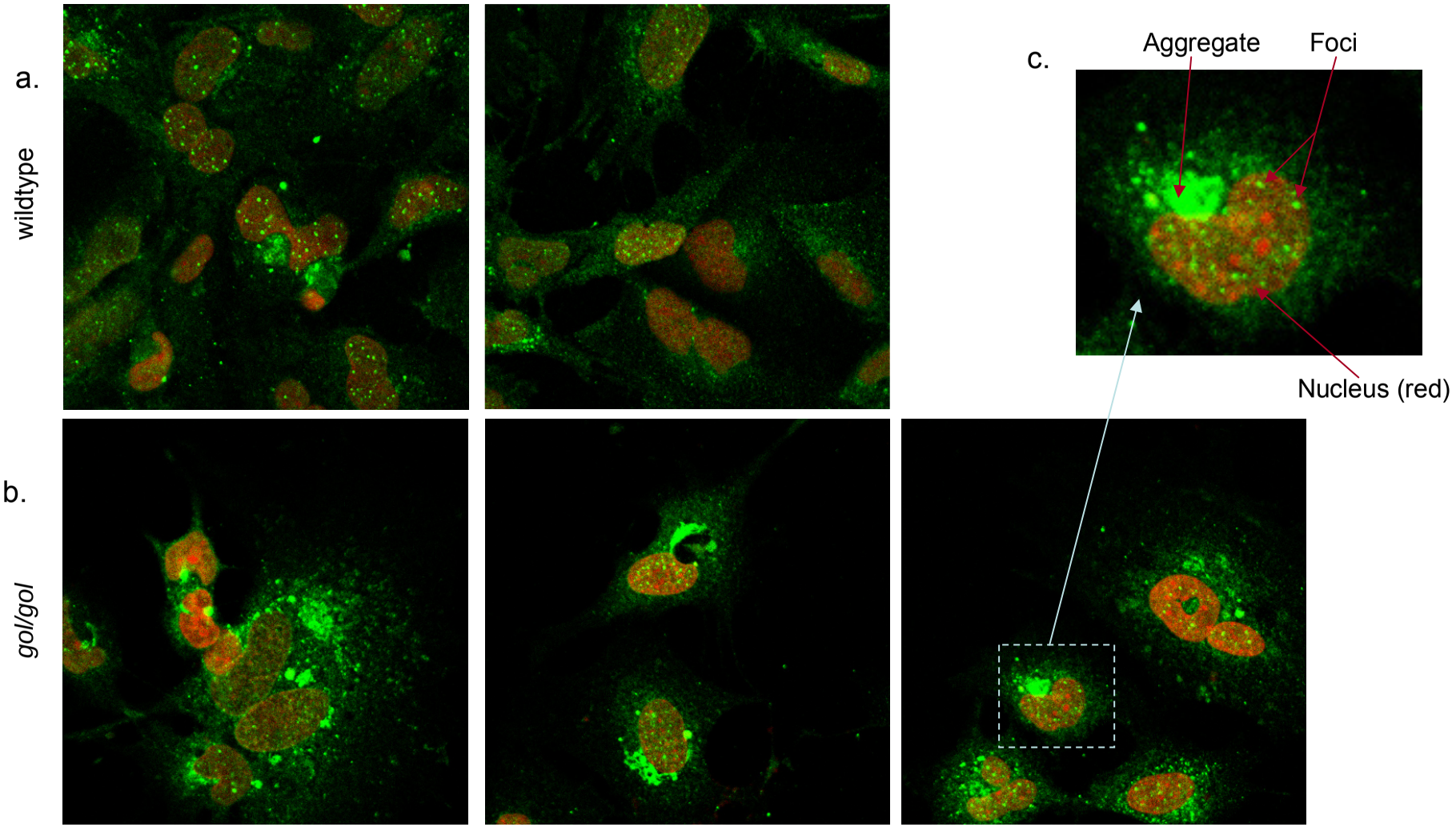

Figure 5.12: Nuclear localization of Brca1 in *gol/gol* and wildtype cells following γ-irradiation.
a. Wildtype cells. **b.** *gol/gol* cells. **c.** Zoom-in on one *gol/gol* cell to show nuclear foci and an aggregate. Brca1 staining is shown in green, nuclear staining with propidium iodide (PI) in red; all images are shown as merges of both stains. Immunlocalization and confocal microscopy were performed by Michal Goldberg (see Methods). The Brca1 antibody M-20 (Santa Cruz) was used.

untreated *gol/gol* cells exhibit aggregates, but they are generally smaller than the aggregates seen in γ-irradiated *gol/gol* cells (inset Figure 5.9). The reason for aggregate formation, or whether they have any functional consequences, is unknown. It is possible that they are a consequence of overexpression of the Brca1^{gol} protein, or may indicate that Brca1^{gol} is more stable than wildtype Brca1 or degraded inefficiently. As only one antibody was used in these immunolocalization studies, it is additionally possible that the aggregates are an artifact of this antibody, although such aggregates were not reported by another group using the same antibody (Bachelier, 2000).

5.3 DISCUSSION

5.3.1 Brca1^{gol} and base repair

This chapter describes a series of experiments designed to investigate the response of *gol/gol* ES cells to various forms of DNA damage. It was first shown that *gol/gol* cells have a colony-forming ability comparable to that of wildtype cells following UV irradiation or oxidative stress from exposure to H_2O_2.

There are several indications that BRCA1 is involved in the response to base damage. One is the reaction of the protein to these types of damage – BRCA1 appears to be modified by phosphorylation and dispersed from normal S phase foci following UV or H_2O_2 exposure (Scully, 1997b; Thomas, 1997; Okada and Ouchi, 2003). Experimental evidence indicates a role for BRCA1 in transcription-coupled repair (TCR) of oxidative damage. 8-oxo-guanine lesions are generally repaired by base excision repair (BER), but repair of the mutation in actively transcribed genes occurs through a TCR pathway (Le Page, 2000a). Human HCC1937 cells, which lack both wildtype BRCA1 and p53, appear to be deficient in TCR of an 8-oxo-guanine lesion transfected into the cells on a plasmid. Adenoviral-based overexpression of *BRCA1* rescues this TCR defect (Le Page, 2000b). *Brca1*$^{\Delta X.11/\Delta X.11}$ ES cells (allele described in Table 1.3 #5) appear to be hypersensitive to oxidative damage from H_2O_2 exposure, and *Brca1*$^{\Delta X.11/\Delta X.11}$*, p53*$^{-/-}$ MEFs are also

hypersensitive to H_2O_2 exposure compared to *Brca1*$^{+/\Delta X.11}$, *p53*$^{-/-}$ MEFs. Some evidence indicates that this may result from a TCR deficiency (Gowen, 1998; Cressman, 1999a; Gowen, 2003).

These *Brca1*$^{-/-}$, *p53*$^{-/-}$ MEFs may also be more sensitive to UV exposure when compared to *Brca1*$^{+/-}$, *p53*$^{-/-}$ MEFs (the difference was not statistically significant at all doses tested) (Cressman, 1999a). The involvement of BRCA1 in global genomic repair (GGR) of UV-induced lesions has been suggested by an experiment involving tetracycline-controlled overexpression of *BRCA1* in *p53*$^{+/+}$ or *p53*$^{-/-}$ human cell lines (Harkin, 1999). In *p53*$^{-/-}$ cells, UV-induced lesions are repaired efficiently by TCR, but cannot be repaired by GGR. When *BRCA1* was overexpressed in *p53*$^{-/-}$ cells, UV-induced lesions on the non-transcribed strand were repaired efficiently. Overexpression of *BRCA1* in *p53*$^{+/+}$ cells did not significantly change the amount of repair on either strand (Hartman and Ford, 2002).

Data generated using the *gol/gol* ES cells contrasts with the studies described above, which may indicate either that the N-terminal region mutated in Brca1^{gol} is not required for the response of cells to base damage (i.e., triggering cell-cycle checkpoints or aiding in the actual repair) or that the *gol* mutation allows the cell to ignore or tolerate mutated bases. However, if it is the case that the *gol/gol* cells are able to ignore base damage, it might be expected that these cells would appear to be hyposensitive to damage at higher doses compared to wildtype cells. This was not observed. The lack of hypersensitivity to base damaging agents may be somewhat surprising, as damaged bases are capable of generating double-strand breaks in following replication errors or polymerase stalling. For this reason, it would be worthwhile to determine the cell-cycle kinetics of the *gol/gol* cells both before and after DNA damage to determine if they undergo cell-cycle arrest as would normally occur. If undamaged mutant cells normally have a delay in S phase progression, then UV-irradiated mutant cells may appear to have a normal repair response simply because the delay allows additional time for repair. Figure 5.1b suggests that such a delay is not taking place, but BrdU labeling

of the cells to confirm that S phase is occurring normally should be done to support these data further.

It should also be noted that, in contrast to previous studies of the involvement of Brca1 in the response to base damage, *gol/gol* cells do not have known secondary mutations. This may be a relevant point, because *p53*-deficient cell lines are known to have a deficiency in GGR of UV-induced damage (Hartman and Ford, 2002), and p53 upregulates several genes (including *p21*) following UV exposure (el-Deiry, 1993). While *p53*-deficient cells are only slightly hypersensitive to H_2O_2 treatment (Yin, 1998; Lin, 2000), p53 is stabilized and upregulates *p21* in response to H_2O_2 treatment (Chen, 2003). BRCA1 can also upregulate *p21* in response to DNA damage, in a p53-independent manner, and overexpression of *BRCA1* has been shown to upregulate *p21* expression (Somasundaram, 1997; MacLachlan, 2000b). It is therefore possible that the hypersensitivity of cells lacking p53 and BRCA1 (such as the HCC1937 cell line or the *Brca1*$^{-/-}$, *p53*$^{-/-}$ MEFs described above) to UV irradiation or H_2O_2 exposure is due at least in part to loss of p53, and that expression/overexpression of *BRCA1* rescues the phenotype by independently activating *p21*.

5.3.2 Brca1^{gol} and DSBR

gol/gol ES cells are hypersensitive to MMC and γ-irradiation, both of which cause lesions repaired by the DSBR pathway. These results are consistent with numerous other studies confirming the involvement of BRCA1 in DSBR (reviewed in Jasin, 2002; Thompson and Schild, 2002). The consistent phenotype of γ-irradiation hypersensitivity in *BRCA1*-mutant cells, regardless of the area mutated, has led to the suggestion that multiple domains of BRCA1 are necessary for the response to this mutagen (Scully, 1999). As BRCA1 has been linked to both HRR and NHEJ, the efficiency of both of these processes in *gol/gol* ES cells was queried.

5.3.2.1 gol/gol cells and HRR

Various assays have been used to assess HRR in cell lines, including I-SceI assays, PFGE-monitored repair kinetics following DNA damage, and gene-targeting in cells.

The I-SceI system has the advantage that it measures repair of an induced DSB, modeling a damage-induced break in the genome, and several groups have demonstrated that ability to repair an I-SceI break parallels the radiation-sensitivity of the cell line (Johnson and Jasin, 2001). However, it is acknowledged that the break generated may not be the most accurate model of a radiation-induced DSB: the I-SceI endonuclease generates a directly re-ligatable set of 4-bp overhangs which retain their 3' hydroxy groups; DSBs generated by γ-irradiation are likely to be more diverse and include blunted ends as well as ends lacking hydroxy groups (Willers, 2002). Pulsed-field gel electrophoresis (PFGE)-based monitoring of DBS repair following damage can be used to assess the overall amount of repair, and has the advantage that it can be used to measure the kinetics of repair of radiation-induced breaks.

Gene targeting can also be used as an assay for the efficiency of homologous recombination, but has the disadvantage of not measuring repair of an induced break in the genome. In the mouse, proving that HRR genes are involved in gene targeting is not completely straightforward, as many of the key genes involved generate embryonic lethal mouse knockouts (*Rad51, Rad50, Mre11*) (Lim and Hasty, 1996; Xiao and Weaver, 1997; Luo, 1999). However, *Rad54* knockout mice are viable. *Rad54*$^{-/-}$ ES cells are hypersensitive to DSB-inducing agents such as γ-irradiation and MMC, and gene targeting is markedly decreased in these cell lines (7-10 fold, using 2 targeting vectors) (Essers, 1997). *Rad52*-deficient mice are also viable. *Rad52*$^{-/-}$ ES cells are not hypersensitive to ionizing radiation, and have only a slight decrease in targeting efficiency (Rijkers, 1998). These data suggest that targeting efficiency may be linked to radiation sensitivity, and supports the use of gene targeting as an assay for HRR. However, it is possible that that

an overlapping yet distinct set of proteins mediate homology-directed repair and homology-directed integration of targeting vectors.

gol/gol ES cells have a slight decrease in homologous recombination efficiency as measured by gene targeting (Figure 5.7). A deficiency in homologous recombination is in agreement with several similar studies using *Brca1*$^{\Delta X.11/\Delta X.11}$ ES cells (allele described in Table 1.3 #5) (Moynahan, 1999; Moynahan, 2001). The ES cells used by Moynahan *et al.* appear to be more severely deficient in homologous recombination than are *gol/gol* ES cells; the former had almost undetectable gene-targeting efficiencies compared to wildtype or heterozygous cells, with a 13-fold difference in targeting efficiencies once random integration was factored in. *gol/gol* ES cells showed a more modest 1.2- to 5.6-fold decrease compared to wildtype cells (Moynahan, 1999; Moynahan, 2001). However, when Moynahan *et al.* used an I-SceI assay to measure the repair of DSBs by HRR, their mutant cells were 5- to 6-fold less efficient at repair than wildtype cells. The results of this assay correlate well with the results generated using *gol/gol* ES cells (Moynahan, 1999). However, there is a difference between the gene targeting efficiencies of the two *gol/gol* mutant cell lines used in the assays, something that promotes consideration of another assay for confirming the results.

5.3.2.2 gol/gol cells and NHEJ

NHEJ is commonly assessed by one of several methods – I-SceI rejoining, direct integration of plasmids, plasmid-based transfection assays (in cells or using cell-free extracts), PFGE-based measurement of repair kinetics, or by measuring the response to retroviral insertion (Daniel, 1999; Moynahan, 1999; Li, 2001; Willers, 2002; Zhong, 2002a; Zhong, 2002b). Although the I-SceI assay again has the advantage of being break-induced, this assay generally involves selection of a reconstituted selection cassette. Error-prone NHEJ generally will not reconstitute such a cassette, meaning that amplification/sequencing of the cassette (or some other method of physical determination) must be carried out to determine if rejoining has occurred. Additionally, accurate NHEJ may be classified as HRR if selection of a

reconstituted cassette is used (Willers, 2002). Plasmid substrates, used in cell-free or *in vitro* assays, also commonly need to be recovered for analysis, and these substrates may be subject to nuclease attack when introduced into cells.

Random integration of a linearized plasmid carrying a selection marker into the genome of cells has also been used to assess the efficiency of NHEJ. This assay has the disadvantage of not measuring the response to a damage-induced DSB. However, there are indications that integration of a plasmid into the genome utilizes the key proteins in NHEJ (although other factors are also likely to be involved). Insertion of the linearized vector is assumed to take place at a DSB in the genome. This supposition is supported by early studies which demonstrated that insertion of a plasmid does not take place at genomic sites carrying any homology to the insert. Instead, insertion sites showed microhomologies (1 or 6 bp) at the joining junction, or short deletions, both of which are consistent with the mechanism of NHEJ (Murnane, 1990; Lieber, 2003). Further, sequencing-based studies of repair at induced genomic breaks (I-SceI sites) showed that about 8% of repaired sites had "captured" extrachromosomal DNA – either part of the I-SceI expression plasmid itself, or, in a second study, ΦX174 fragments introduced into the cell with the I-SceI plasmid. Integration appeared to occur preferentially at the induced break-site and not elsewhere in the genome. Again, microhomologies of 1-4 base pairs were commonly seen at insertion sites, along with small deletions at the junctions (Lin and Waldman, 2001; Dellaire, 2002). Functional data generated using knockout cell lines also supports the idea that random integration of linear plasmids requires key NHEJ proteins: cell lines lacking DNA-PKcs (mouse scid lines), Ku80 (hamster xrs5), Nbs1 (mouse ES knockout cell line), or XRCC4 all have a lower efficiency of genomic integration of linear plasmids compared to wildtype cells. None of the cell lines tested appeared to have a lowered transfection efficiency (Harrington, 1992; Manivasakam, 2001; Willers, 2002; Zhang, 2004). In the case of the Nbs1-mutant ES cell line, expression of an *Nbs1* transgene restored the efficiency of plasmid integration (Zhang, 2004). For each of the genes listed above, the cell line (or mouse model) has a V(D)J recombination

deficiency (or is immunodeficient) and shows hypersensitivity to DSB-inducing agents, indicating that lack of these genes correlates with repair-related and V(D)J-related NHEJ (Biedermann, 1991; Pergola, 1993; Errami, 1998; Gao, 2000; Kang, 2002).

NHEJ in *gol/gol* ES cells was assessed by integration of a selectable cassette into the genome. Data reported in this chapter suggest that *gol/gol* ES cells have an elevated efficiency of NHEJ compared to wildtype cells, which agrees with several previous studies The majority of studies using the human HCC1937 cell line showed that these cells do not appear to have a defect in NHEJ (Table 1.5). A recent experiment done using HCC1937 cells gave results very similar to the ones generated in this study: plasmid integration in HCC1937 cells was increased compared to wildtype cells. Addition of a *BRCA1* transgene to the cells brought the integration frequency back to wildtype levels (Zhang, 2004). In the *Brca1*$^{\Delta X.11/\Delta X.11}$ murine ES cells studied by Moynahan *et al*., the efficiency of NHEJ was elevated. This elevation was corrected by addition of a *Brca1* transgene, indicating that the change was likely due to the loss of *Brca1* (Moynahan, 1999; Snouwaert, 1999). These same cells have been assayed for NHEJ using the I-SceI assay. The result of the two assays, while not identical in fold-difference, show the same general trend of increase or decrease (Moynahan, 1999; Moynahan, 2001; Zhong, 2002a).

In contrast to the results in this chapter, several experiments have indicated that *Brca1*$^{-/-}$*, p53*$^{-/-}$ MEFs have a lower efficiency of NHEJ as compared to that of *p53*$^{-/-}$ MEFs (allele described in Table 1.3 #4) (Zhong, 2002a; Zhong, 2002b). The reason for this difference is not clear, but some of the assays performed on these MEFs indicate that they may have a defect in precise end joining but not in overall end-joining. This observation is supported by a recent study which showed that lymphoblastic cell lines generated from breast-cancer patients who carry a *BRCA1* mutation have a deficiency in precise end-joining, although their overall end-joining is similar to that of lymphoblast cell lines derived from healthy control individuals (Baldeyron, 2002). However, there is a possibility that the *Brca1*$^{-/-}$*, p53*$^{-/-}$ MEF line

carries other mutations, and that the cell lines derived from adult cancer patients may also have secondary mutations. It is difficult to compare the results generated using *gol/gol* ES cells with data from *Brca1*$^{-/-}$, *p53*$^{-/-}$ MEFs, as *gol/gol* cells were assessed only for the efficiency of overall end-joining, not for the precision with which they repair a break.

5.3.2.3 gol/gol cells: difference between cell lines

Data presented in Figures 5.7 and 5.8 indicates that the *gol/gol* ES cell lines perform consistently between assays, but they are noticeably different when compared to one another. This may indicate that there are secondary mutations in one cell line vs. the other, and perhaps the use of SKY, chromosome banding, or CGH array (readily available in the lab) would be of use in assaying for any gross rearrangements in the genome of these cell lines. The use of other assays, such as the I-SceI assay or PFGE is desirable and should highlight if the cell-line difference is a real effect or not. The only problem that might arise from use of the I-SceI assay (although a substrate might be designed to get around this problem) is that if accurate NHEJ is elevated in the *gol/gol* cells and HRR is depressed, NHEJ events might be scored as HRR events and lead to wildtype and mutant cells having little overall difference. This concern may be unfounded, as the accuracy of NHEJ in *gol/gol* cells has not been measured. PFGE-based monitoring of break repair following damage might also be used. Since the change in the kinetics of damage repair can be used to determine which form of DSBR is non-functional, this assay (done over a range of doses) might more clearly define the repair defects of the *gol/gol* cells. Before doing either of these assays, it would be useful to look at the cell-cycle kinetics of *gol/gol* ES cells following DSB-related DNA damage; the results of such a study should indicate if blockage/loss of checkpoint control occurs following damage.

5.3.2.4 In summary

The elevation of NHEJ efficiency and slight decrease in HRR efficiency in *gol/gol* cells may describe a mechanism by which Brca1 contributes to tumourigenesis: an increase in error-prone repair coupled to a backlog of unrepaired lesions. This idea correlates well with the expression levels of

Brca1; it is a protein expressed maximally in S and G2/M phases, phases in which HRR is thought to be the major repair pathway (Ruffner and Verma, 1997; Scully, 1997b). Whether this means that the *gol/gol* ES cells have a defect in normal or break-induced cell cycle phase distribution has yet to be determined. The question of why an increase in NHEJ would not phenotypically "rescue" the HRR deficiency is answered by several studies indicating that the two forms of repair do not complement one another. A previous study using mice deficient for either *Rad54* (involved in HRR) or the gene encoding DNA-PKcs (*scid*, essential for NHEJ) demonstrated that *Rad54*$^{-/-}$, *scid*$^{-/-}$ double knockout mice were more hypersensitive to γ-irradiation than mice deficient for only one gene (Essers, 2000). Additionally, *Rad54*$^{-/-}$ or *Ku70*$^{-/-}$ (NHEJ deficient) chicken DT40 cells have been used to demonstrate that *Rad54*$^{-/-}$ cells are γ-irradiation sensitive in late S and G2 phases, while *Ku70*$^{-/-}$ cells are sensitive to γ-irradiation in G1 and early S phases. Cells lacking both genes are more sensitive to γ-irradiation than cells lacking only one gene (Takata, 1998; Wang, 2001b). While the major defect in *gol/gol* cells appears to involve NHEJ, their small decrease in HRR efficiency may also be significant. Previous studies using *scid*$^{-/-}$ fibroblasts have shown that these cells are not hypersensitive to MMC, while cells lacking *Rad54* (and *gol/gol* cells) are hypersensitive to MMC (Biedermann, 1991; Hendrickson, 1991; Essers, 2000). This suggests that at least some of the phenotypes observed in *gol/gol* cells may be attributable to their HRR deficiency.

Experiments described in this chapter also confirm the previous observation that while human tumour cell lines heterozygous for a *BRCA1* mutation appear to be more susceptible to γ-irradiation or MMC than wildtype cell lines, mouse heterozygous-mutant cell lines are not (Figures 5.4, 5.5 (Abbott, 1999; Foray, 1999; Moynahan, 2001)). It is possible to take this observation as an argument that human and murine carriers of *BRCA1* mutations have different cancer predispositions or that human *BRCA1* is a haploinsufficient gene. Perhaps a more logical conclusion is that studies of human tumour cell lines heterozygous for *BRCA1* mutations may be affected by other mutations

carried by these cells, although some human *BRCA1* mutations may well be haploinsufficient.

5.3.3 Immunolocalization of Brca1^{gol}

Immunolocalization studies indicate that Brca1^{gol} is able to localize to the nucleus and appears to form S phase nuclear foci. These results have implications for the interaction of Brca1^{gol} with other proteins, as well as on its biology, which will be discussed further in Chapter 6. However, the level of cytoplasmic localization of Brca1, while consistent between the wildtype and mutant cell lines, is higher than is generally seen, and the overall pattern is more punctate than is generally seen. In order to rule out non-specificity of the antibody being mistake for cytoplasmic localization, the immunolocalization experiments should be redone either with a different antibody, or in conjunction with a peptide which acts as competitor for the antibody.

Following both γ-irradiation and UV exposure, a similar percentage of both wildtype and *gol/gol* cells exhibit Brca1 nuclear foci (Table 5.1). As nuclear foci are also observed in undamaged *gol/gol* cells, this suggests that the N-terminal domain predicted to be missing in Brca1^{gol} is not required for the formation of either normal or damage-induced nuclear foci. However, the amount of focus formation may be lower than it appears, as the overall punctate appearance of the immunolocalization pattern may lead to an overestimation of foci formation. Previously, it was shown that damage-induced foci will form in MEFs carrying the ΔX.11 form of Brca1, but that a version of the human BRCA1 protein lacking part of the C-terminus does not form such foci (Zhong, 1999; Wu, 2000; Huber, 2001). Taken together with data generated from *gol/gol* cells, this suggests that only the C-terminus may be required for the formation of nuclear foci. However, this hypothesis is contradicted by the results of Chiba and Parvin, who overexpressed a version of the human BRCA1 protein lacking residues 1-302 (lacking the RING domain and the NES) and found it did not form normal S phase foci. Additionally, when they overexpressed a mutant form of BRCA1 lacking the

C-terminal BRCT repeats, S phase BRCA1 nuclear foci were observed (Chiba and Parvin, 2002). It is possible that overexpression of the mutant proteins in their study may have resulted in aberrant localization or incorrect protein folding, leading to the discrepancy between these results and the others described above.

Hyperphosphorylation of BRCA1 following DNA damage appears to be the major impetus for dispersion of the protein from normal S phase foci and re-formation into damage-induced foci. While the phosphorylation status of Brca1^{gol} was not investigated, all known phosphorylation sites in the Brca1 protein are downstream of the region deleted by the *gol* allele and are expected to be intact in the Brca1^{gol} protein, suggesting that regulation by this mechanism would still occur (Rosen, 2003). This supposition is supported by the fact that *gol/gol* cells appear to exhibit both S phase and damage-induced nuclear foci in a percentage of cells observed (Figures 5.9 – 5.12, Table 5.1).

A percentage of both non-treated and γ-irradiated *gol/gol* cells have large aggregates of protein, which are rarely seen in γ-irradiated wildtype cells, or in UV-treated wildtype or *gol/gol* cells (inset Figure 5.12 and Table 5.1). The presence of protein aggregates in *gol/gol* cells may indicate that Brca1^{gol} is overexpressed, less soluble, or more stable compared to wildtype Brca1. The stability/overexpression of the Brca1^{gol} protein will be discussed further in Chapter 6. Although aggregates are observed in some γ-irradiated wildtype cells, they are not observed as frequently (Table 5.1). Perinuclear localization of a subtype of phosphorylated BRCA1 has been reported by one group (following UV or γ-irradiation-induced DNA damage in the human MCF7 cell line) (Okada and Ouchi, 2003), and perinuclear concentration of BRCA1 in a human breast cancer cell line has been seen (De Potter, 1998). However, these are not commonly reported findings, and aggregates not been reported previously in studies of Brca1 immunolocalization, including one in which the same antibody was used (Bachelier, 2000). This suggests that they are not likely to be an antibody artifact. They could be a result of using randomly-differentiated cells (which have also not been used in previous studies). To address these concerns, it would be highly desirable to use *gol/gol* MEFs (if

they can be generated) in these studies instead of the differentiated cells, as well as an additional antibody or peptide-competition in conjunction with the M-20 antibody.

5.3.4 Summary

The use of *gol/gol* ES cells has helped to further define the role of Brca1 in the response to DNA damage. Data generated using these cells support several previous observations, help to clarify the role of Brca1 in NHEJ, and indicate that the N-terminus of Brca1 may not be required for base repair or the formation of normal or damage-induced nuclear foci. The molecular characterization of the *gol* allele will be discussed in Chapter 6.